

Integral Equations and Machine Learning

Alexander Keller¹, Ken Dahm²

NVIDIA, Fasanenstr. 81, 10623 Berlin, Germany

Abstract

As both light transport simulation and reinforcement learning are ruled by the same Fredholm integral equation of the second kind, reinforcement learning techniques may be used for photorealistic image synthesis: Efficiency may be dramatically improved by guiding light transport paths by an approximate solution of the integral equation that is learned during rendering. In the light of the recent advances in reinforcement learning for playing games, we investigate the representation of an approximate solution of an integral equation by artificial neural networks and derive a loss function for that purpose. The resulting Monte Carlo and quasi-Monte Carlo methods train neural networks with standard information instead of linear information and naturally are able to generate an arbitrary number of training samples. The methods are demonstrated for applications in light transport simulation.

Keywords: Integral equations, reinforcement learning, artificial neural networks, Monte Carlo and quasi-Monte Carlo methods, light transport simulation, path tracing, light baking, image synthesis.

1. Introduction

The fast progress in the field of machine learning is becoming increasingly important for other research areas including Monte Carlo methods and especially computer graphics. In fact the fields are closely related in a mathematical sense: Reinforcement learning has been shown equivalent to solving Fredholm integral equations of the second kind [1] and is used for simple and efficient importance sampling in light transport simulation. Furthermore, the process of sampling light transport paths from path space to simulate light transport has similarities to the process of computers playing games, as in fact, sampling paths in search trees amounts to playing random games to learn about winning chances [2].

The utility of importance sampling enabled by high-dimensional function approximation by artificial neural networks [3] has recently been demonstrated

¹keller.alexander@gmail.com

²ken.dahm@gmail.com

in an impressive way for learning and playing the game of Go [4], bringing together the aforementioned domains even closer.

We therefore briefly review the equivalence of reinforcement learning and Fredholm integral equations of the second kind in Sec. 2 and point out further analogies to recent advances in machine learning for playing games in Sec. 3. We then derive a scheme to train artificial neural networks within integral equations in Sec. 4 and explore applications in computer graphics: In Sec. 5 a combination of temporal difference learning and artificial neural networks is used for importance sampling light sources and Sec. 6 investigates the feasibility of high-dimensional approximation by artificial neural networks for real-time rendering.

2. Importance Sampling by Reinforcement Learning

Physically based rendering [5] in principle consists of summing up the contributions of light transport paths that connect the camera with the light sources. Due to the large state space, finding contributing paths may be inefficient, for example, because visibility needs to be sampled and is not known up front.

Using reinforcement learning to learn where light is coming from [1] allows for efficient importance sampling of light transport paths. The method has been derived by matching terms of the Q-learning [6] and light transport equations:

$$\begin{aligned}
 Q'(s, a) &= (1 - \alpha) \cdot Q(s, a) + \alpha \cdot \left(r(s, a) + \gamma \int_{\mathcal{A}} \pi(s', a') Q(s', a') da' \right) \\
 L(x, \omega) &= L_e(x, \omega) + \int_{\mathcal{S}_+^2(x)} f_s(\omega_i, x, \omega) \cos \theta_i L(h(x, \omega_i), -\omega_i) d\omega_i \quad (1)
 \end{aligned}$$

In Q-learning, the value $Q(s, a)$ of taking an action a in state s is learned by taking the fraction $1 - \alpha$ of the current value and adding the fraction α of the reward $r(s, a)$ received when taking action a . In addition, all future reward is discounted by a factor of γ . It is determined by the integral over all actions a' that can be taken from the next state s' that is reached from state s by taking action a is computed over the values $Q(s', a')$ weighted by a so-called policy function $\pi(s', a')$.

While this may sound abstract at first, matching the terms with the integral equation describing radiance transport immediately shows the parallels between reinforcement learning and light transport: In fact the reward corresponds the radiance L_e emitted by the light sources, the discount factor times the policy function corresponds to the reflection properties f_s (also called the bidirectional scattering distribution function), telling how much radiance is transported from direction ω_i to direction ω_r through the point on a surface x . The value Q then can be matched with the radiance L that comes from the point $h(x, \omega_i)$ hit by tracing a ray along a straight line from x into direction ω_i and the state space \mathcal{A} corresponds to the hemisphere $\mathcal{S}_+^2(x)$ aligned by the normal in point x . This leaves us with an action a corresponding to tracing a ray.

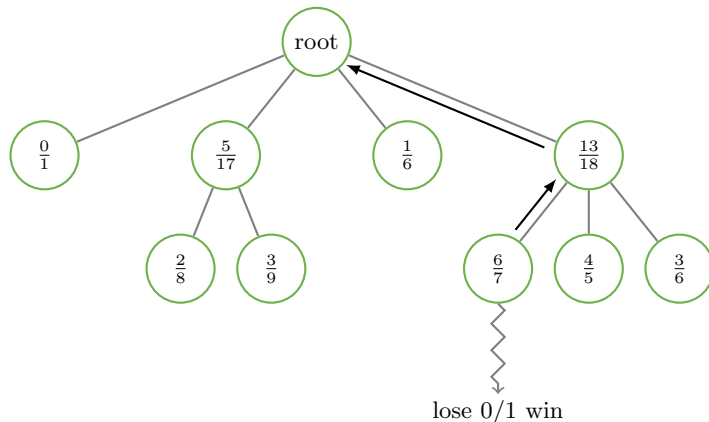


Figure 1: Illustration of the principle of Monte Carlo tree search to find the most valued move represented by the branches from the root node: All children contain a fraction, where the denominator counts the number of visits to the node and the nominator is the reward. In order to update the values, a move is selected considering the values of the children of a node until a leaf node is reached. Unless this leaf node is expanded (see main text), random moves are taken (zig-zag line) until a terminal state of the game is reached. Then the nodes along the path back to the root (along the arrows) are updated by incrementing the number of visits and also incrementing the reward unless the random game has been lost.

Combining both equations yields

$$\begin{aligned}
 Q'(x, \omega) &= (1 - \alpha)Q(x, \omega) \\
 &+ \alpha \left(L_e(y, -\omega) + \int_{S_+^2(y)} f_s(\omega_i, y, -\omega) \cos \theta_i Q(y, \omega_i) d\omega_i \right)
 \end{aligned}
 \tag{2}$$

where Q now represents the incident radiance, which can be learned over time and be used for importance sampling directions proportional to where most light is coming from, i.e. guiding path towards the light sources. The implementation of such algorithms is detailed in [1].

Besides the structural identity of reinforcement learning and a Fredholm integral equation of the second kind, there are more analogies: While Q -learning considers the value of the next, non-terminal state, which corresponds to scattering in transport simulation [1], temporal difference learning [7] is related to next event estimation, and as such deals with terminal states as discussed in Sec. 5.

3. Importance Sampling in Monte Carlo Tree Search

When a computer program needs to decide, which next move in a game is best, it does so by computing a value for each possible move and then uses a heuristic to select the best one. Implementing the rules of a game, it is straightforward to describe the tree, where each path corresponds to the sequence of

moves of one complete game. As for most interesting games this tree is growing exponentially with the number of moves, building such a tree is not feasible for most games and hence various tree search heuristics have been explored.

The currently most powerful algorithms [4] are based on Monte Carlo tree search as illustrated in Fig. 1. Instead of trying to evaluate the complete search tree, the key principle is to estimate the value of a move by randomly sampling a path in the search tree and counting how often such random games are won. Repeating the procedure the statistics can be improved, while the running time stays linear in the maximal number of possible moves of the games. Note that randomly selecting moves in a game resembles selecting random scattering directions in light transport simulation to generate light transport paths.

In order to increase the efficiency of Monte Carlo tree search, parts of the search tree may be stored as illustrated in Fig. 1. Nodes then store their total number of visits n and the reward w , when passing through them. Whenever a node is reached during tree traversal that is not the terminal node of a game, children may be appended to count results of the random tree exploration. While the number of stored nodes is bounded by available memory, there are additional heuristics to only create new nodes once their parents have a sufficiently high value and number of visits.

3.1. Action Selection and Simulation of Densities

When selecting an action, i.e. a move in the game, exploration and exploitation are competing goals. On the one hand, the tree search needs to be able to simulate all possible games in order to learn. On the other hand, game play should be strong and highly valued moves should be preferred. This balance is achieved by computing the so-called upper confidence bound [8]

$$u = \frac{w}{n} + c \cdot \sqrt{\frac{\ln N}{n}},$$

for each possible move for the current state. The value $\frac{w}{n}$ of games won passing through the node under consideration accounts for exploitation, as it is large for likely good moves. With N being the total number of simulated games, the second term remains large for nodes that have not been visited often. With the constant c usually set to $\sqrt{2}$, this term ensures exploration. As long as all values are available, the next move is selected as the child with maximum u value during Monte Carlo tree search.

This method overcomes previous methods like, for example, ϵ -greedy action selection, which would just choose the child with maximal $\frac{w}{n}$, unless a random number is less than a threshold ϵ , in which case a random action would be taken. As it is very close to what can be done in reinforcement learned importance sampling in light transport simulation, we mention probabilistic action selection, which assigns the probability

$$\text{Prob}(a_i | s) = \frac{TQ(s, a_i)}{\sum_{a_k} TQ(s, a_k)} \quad (3)$$

to each possible action a_i . Then a small T favors exploration, while large T tend to exploitation. Starting with a small T during learning, the probabilities remain more uniform, while with growing T actions with higher value will become selected as the values Q become more reliable.

Action selection in reinforcement learned importance sampling in light transport simulation amounts to sampling a direction proportional to Q (see Eqn. 2) rather than selecting the maximum of a distribution.

Guaranteeing that exploration always remains possible corresponds to guaranteeing ergodicity in transport simulation. Hence all densities and values are required to be non-zero as long as there may be a non-zero contribution of a path.

3.2. Artificial Neural Networks for Densities and Values

While random play is feasible, it is not really efficient when a large number of samples is required in order to achieve reliable values for action selection. Especially for large state or action spaces this may become a bottleneck. Using expert knowledge can improve the selection process [9], but requires the acquisition and formalization of such knowledge.

Reinforcement learning and self-play [10, 4] have been demonstrated to overcome these issues. In analogy to reinforcement learned importance sampling in light transport simulation [1], key to efficiency is guiding the paths in the search tree along the most rewarding nodes even during random play, where no information has been stored, yet. As discrete representations are not feasible due to the size of the state space alone, deep artificial neural networks [3] have been trained to predict the values of moves. In Sec. 5 and Sec. 6, we discuss artificial neural networks to replace discrete representations in light transport simulation.

4. Training Artificial Neural Networks within Integral Equations

The artificial neural networks in [4] are trained by self-play, where reinforcement learning is realized by having the computer play against itself. This is possible by Monte Carlo tree search exploring random games according to the rules of the game as described in Sec. 3.

Now light transport is ruled by the Fredholm integral equation (1) and training an artificial neural network requires an error, a so-called loss function. This error is derived by taking a look at Eqn. (2): Assuming that learning has converged, meaning $Q' = Q$, yields $\alpha = 1$ and hence

$$Q(x, \omega) = L_e(y, -\omega) + \int_{S_+^2(y)} f_r(\omega_i, y, -\omega) \cos \theta_i Q(y, \omega_i) d\omega_i.$$

Representing $Q(x, \omega)$ by an artificial neural network $\hat{Q}(x, \omega)$ [3], lends itself to defining the error

$$\Delta Q(x, \omega) := \hat{Q}(x, \omega) - \left(L_e(y, -\omega) + \int_{S_+^2(y)} f_r(\omega_i, y, -\omega) \cos \theta_i \hat{Q}(y, \omega_i) d\omega_i \right)$$

as the difference between the current value of the network $\hat{Q}(x, \omega)$ and the more precise value as evaluated by the term in brackets. During learning $\Delta Q(x, \omega)$ is used to train the artificial neural network $\hat{Q}(x, \omega)$ by back-propagation [11].

An online quasi-Monte Carlo algorithm for training the artificial neural network $\hat{Q}(x, \omega)$ by reinforcement learning then

- generates light transport paths using a low discrepancy sequence [12] and
- for each vertex of a path evaluates $\Delta Q(x, n)$ to
- train the artificial neural network $\hat{Q}(x, n)$ by back-propagation.

Other than the classic training of artificial neural networks, the training set is infinite and in fact each generated path is unique and used for training exactly once. As any number of training samples can be generated by a deterministic low discrepancy sequence, the samples are perfectly reproducible, which allows for efficiently exploring the hyperparameters of the artificial neural network. This method falls in the same class as methods training artificial neural networks without clean data [13]. In fact standard information in the form of samples is used instead of using linear information [14] in the form of functionals of the solution of the integral equation.

5. Learning Next Event Estimation

Recent research [15, 16] has shown that deep artificial neural networks [3] very successfully can approximate value and policy functions in temporal difference learning or reinforcement learning. In physically based rendering, for example path tracing, we need to find efficient policies for selecting good scattering directions or light sources for next event estimation that have high importance.

In order to compute the direct illumination, we have to integrate the radiance L_i over the surfaces of all light sources, i.e.

$$L(x, \omega) = \int_{y \in \text{supp} L_i} L_i(\omega_i, y) f_r(\omega, x, \omega_i) G(x, y) V(x, y) dA_y \quad (4)$$

$$\approx \frac{1}{N} \sum_{i=0}^{N-1} \frac{L_i(\omega_i, y_i) f_r(\omega, x, \omega_i) G(x, y_i) V(x, y_i)}{p(y_i, \omega_i)}, \quad (5)$$

which is estimated by the Monte Carlo method, as in practical settings there is no analytical solution. In order to reduce variance, one of the main challenges is picking the probability density function $p(y_i, \omega_i)$ for light source selection. The obviously best choice is a function proportional to the integrand, however, this is not an option as the visibility term V is expensive to evaluate and discontinuous in nature. We therefore utilize temporal-difference learning [17] to learn the distribution over time, i.e.

$$Q'(s, i) = (1 - \alpha)Q(s, i) + \alpha L_i(\omega_i, y_i) f_r(\omega, x, \omega_i) G(x, y_i) V(x, y_i),$$

where s is the current state, i.e. a discretized location, normal vector, and incoming direction, and i is the light source index. This gives us a temporal average of all contributions we have evaluated so far for certain locations in space. The original temporal difference algorithm discretizes the state and action space in order to compute these averages.

As compared to previous approaches, approximating the function $Q(s, i)$ by an artificial neural network may avoid discretization artifacts and use less memory to store the $Q(s, i)$ values.

5.1. Artificial Neural Network Training and Rendering

Fig. 2 outlines the algorithm, which simultaneously trains an artificial neural network and renders the image. Operating in mini-batches of $M = 64$ quasi-random samples, a ray is traced from the eye through each pixel identified by a sample of the Halton sequence [18] and intersected with the scene geometry to find the closest point of intersection. At this point, a light source for direct illumination is selected and its contribution is computed according to Eqn. (5).

The light source is selected using an artificial neural network, whose input layer consists of nine neurons, receiving the normalized position, normal vector, and incoming direction of the intersection point. The output layer contains as many neurons as there are light sources and provides a Q value for each light source and is realized by the so-called "softmax" activation function [3]. All other layers in the network use rectified linear units (ReLU). Finally, the light source then is selected by sampling using the cumulative distribution function.

The contribution of a light source sample as well as the intersection details are stored in an array and once M mini-batches are complete, we retrain the network using stochastic gradient descent [11].

5.2. Results

Fig. 3 shows the results of an exploratory experiment, where a small artificial neural network with 2 hidden layers of 64 neural units each has been used to learn the light source contribution including visibility. The reduction in variance as compared to uniform light source selection is clearly visible.

5.3. Discussion

The artificial neural network to approximate the importance of a light source including visibility can be trained during rendering or ahead of image synthesis. While the gain in efficiency has been demonstrated in an experiment, there are two major challenges that need to be solved: First, evaluating an artificial neural network per thread on a parallel processor is much more expensive than looking up a value of importance in a table. The second issue is the costly computation of that cumulative distribution function.

Note that when combining next event estimation with path tracing with reinforcement learned importance sampling [1] by multiple importance sampling [19, 20] of course the integrands weighted by the multiple importance sampling weights need to be learned instead of the unweighted ones.

```

Function renderImage()
  initNetwork()
  for  $i = 1$  to  $N$  do
    for  $j = 1$  to  $M$  do
      for  $k = 1$  to 64 do
         $p \leftarrow \text{selectPixel}(\xi_0^{i,j,k}, \xi_1^{i,j,k})$ 
         $x, n, r \leftarrow \text{traceRay}()$ 
         $qs \leftarrow \text{neuralNetwork}(x, n, r)$ 
         $cdf \leftarrow \text{buildCdf}(qs)$ 
         $l \leftarrow \text{sampleCdf}(cdf, \xi_2^{i,j,k})$ 
         $c \leftarrow \text{getContribution}(l)$ 
         $\text{addContributionToImage}(p, c)$ 
         $\text{minibatches}[j][k] \leftarrow x, n, r, l, c$ 
       $\text{retrainNetwork}(\text{minibatches})$ 
   $\text{outputImage}()$ 

```

Figure 2: Pseudocode for rendering direct illumination: An artificial neural network is trained in mini batches during rendering so that over time the light source will be selected proportional to Eqn. (4).

6. Learning Radiance

In computer games lighting has to be computed in real-time. Yet, given the compute power available in a typical game console, physically accurate lighting may only be approximated. Approximating the radiance $L(x, \omega)$ had not been very practical, since the function is not smooth and depends on at least five dimensions, i.e. the three-dimensional location x in space and the direction of observation ω .

Computing and storing parts of the illumination information ahead of game play is common practice. For example, often only the incident indirect radiance is stored for discrete locations x : The radiance incident in such a location has been approximated using spherical harmonics [21] and wavelets [22], although the radiance incident over the sphere usually is neither smooth nor piecewise constant. While such representations are computationally efficient, they require a considerable amount of memory for the coefficients across the locations x . Adaptive data structures [23, 24] are more suitable for offline rendering, as their construction is more costly and involved.

In a similar way, artificial neural networks have been explored to address the curse of dimension in computer graphics: In [25, see Fig.2 and first paragraph in App.A], a 4-layer artificial neural network with 20 hidden neurons in the 2nd and 10 hidden neurons in the 3rd layer has been used to approximate the red, green, and blue components of the indirect radiance given position x , viewing direction ω , both the surface normal n and texture information a in x , as well as the position l_k of the k -th point light source. The radiance of each point

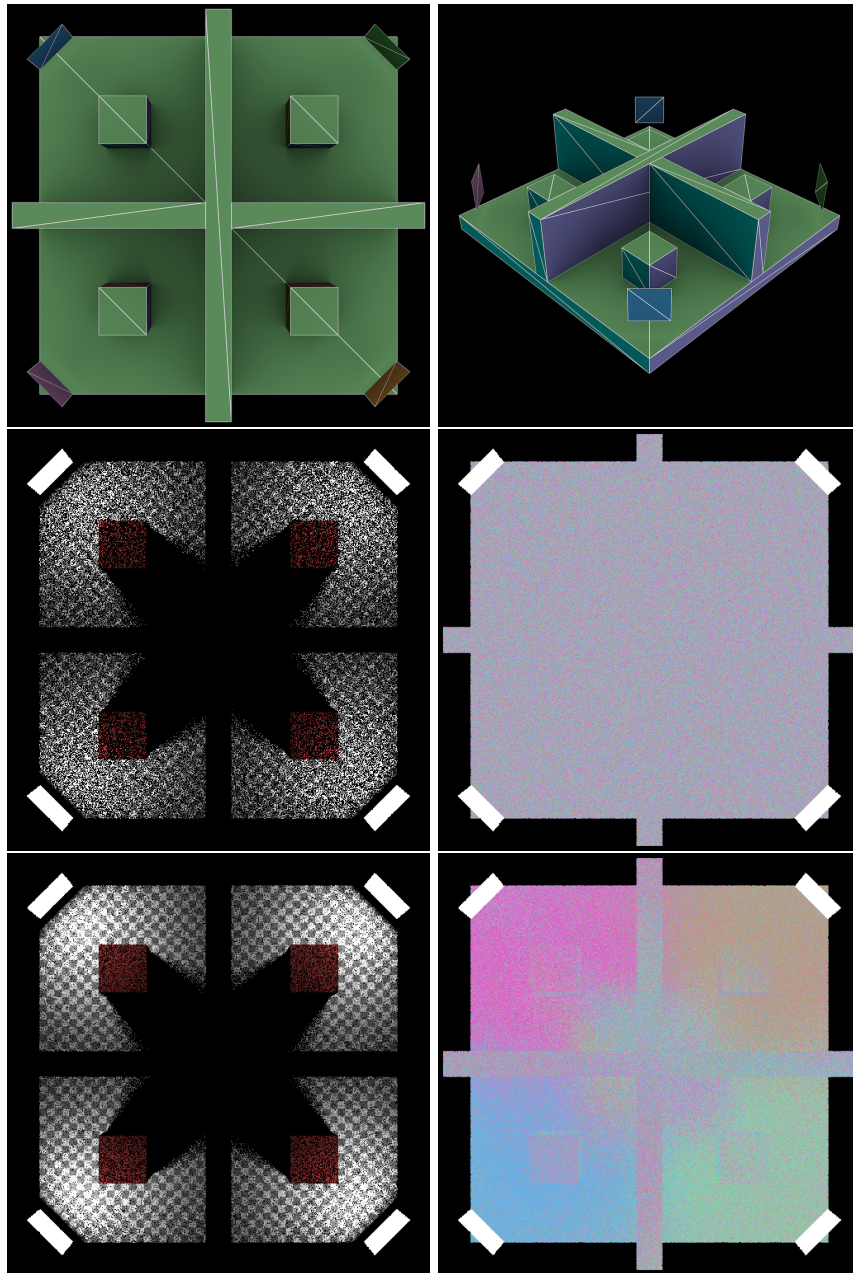


Figure 3: Top row: Geometry of a test scene with eight light sources in four independent rooms, where in each room only two light sources are visible. The other images on the left show the results of uniform light source selection (middle), whereas the bottom image shows the result using an artificial neural network learning the importance of a light source including visibility. The false color visualization on the right illustrates the index of the light source selected, where the color noise in the middle shows uniformly random selection, while at the bottom the clear coloring illustrates that with high probability only visible light sources are picked.

light source is determined by evaluating the artificial neural network multiplied by the point light source color c_k and summed up to approximate the indirect radiance in x .

In [26], the temporally dependent, rather smooth radiance function of a sky illumination model on the sphere has been successfully approximated by a small artificial neural network. In contrast, using one tiny artificial neural network to control the computational cost of the approximation indirect radiance in a complex scene did not work out in [25]: Decreasing the approximation error required to adaptively partition the scene hierarchically using a 3d-tree, where each voxel refers to one artificial neural network. While the evaluation of indirect radiance is close to real-time, finding such a partition and training the artificial neural networks remains very computationally expensive.

6.1. Baking Radiance into an Artificial Neural Network

In order to explore how well tiny artificial neural networks can approximate the solution $L(x, \omega)$ of the radiance integral equation (1) and given the findings of [25] as summarized above, the scene is partitioned into a grid of uniform voxels. In a first step, the surface of the scene is uniformly sampled and for each point on the scene surface the incoming radiance is computed for a selected random direction on the unit hemisphere aligned by the surface normal. The sample’s position in space with its surface normal and the incoming direction as well as the computed radiance value are stored in a training data list associated with the voxel the sample lies in. Then the second step of the algorithm trains a fully connected artificial neural network for each voxel using the stored training data. Finally, given a point in the scene, we approximate its radiance by identifying its voxel and evaluating its associated artificial neural network given the position, normal vector, and incoming direction. In contrast to [25] we train the artificial neural network on the full light transport equation, meaning we approximate direct and indirect illumination at once instead of computing direct illumination separately.

Fig. 4 shows the artificial neural network architecture that is used inside each voxel. It consists of an input layer of nine neurons (i.e. normalized position inside the voxel, normal vector, incoming direction), one hidden layer of nine neurons and an output layer of three neurons for the radiance in the RGB color space. In accordance with [25], Experiments indicate that the more complex the geometry, the more layers and/or neurons are required in order to approximate the radiance $L(x, \omega)$. Hence keeping the artificial neural networks small requires a finer partition of the scene in such situations.

6.2. Results

Fig. 5 compares the approximation by artificial neural networks to a reference image by showing the squared difference. The reference has been path traced with 512 paths per pixel of length six. The scenes have been discretized into $3 \times 3 \times 3$ voxels requiring 27 artificial neural networks. 10000 points have been distributed uniformly across the scene and each point has been inserted into

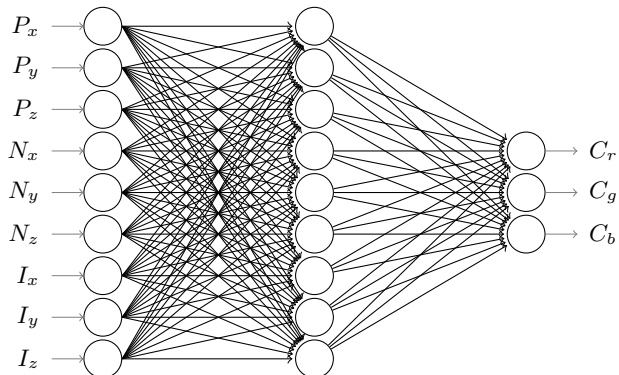


Figure 4: Example of a fully connected artificial neural network as used for the radiance representation inside a voxel. All activation functions are rectified linear units (ReLU). Given position P , surface normal N , and incident direction I , the color C is determined.

its respective voxel together with the computed radiance values after shooting 512 random rays into its local hemisphere. While the approximation is already good at one sample per pixel, 4 samples per pixel were used for anti-aliasing in order to attenuate the approximation error along edges (see the cube silhouette in the error image in Fig. 5). The error images were scaled by a factor of 10, since otherwise differences would be hard to spot qualitatively. In comparison to traditional light baking techniques, view-dependent effects such as glossy reflections can be efficiently approximated by artificial neural networks, which is their most prominent advantage.

6.3. Learning Visibility

In addition to learning the full light transport and as an alternative to Sec. 5, we can also train an artificial neural network to approximate the probability distribution of selecting light sources with high contribution and thus including visibility. During rendering we then feed the intersection details to the network, which in turn yields a probability distribution over the light sources. Building and sampling the cumulative distribution function on-the-fly allows for sampling proportional to this distribution. Fig. 6 shows the result of this method compared to random selection of light sources. With just one sample per pixel we can almost perfectly select a light source. The remaining noise in the image is caused by sampling light sources with a finite area. The algorithm works similar to the one for learning radiance in Sec. 6.1.

6.4. Discussion

Using artificial neural networks for high-dimensional approximation allows for representing both smooth as well as discontinuous parts of the target function and capturing view dependent effects such as for example gloss. Compared to point-wise representations, less memory is required and adaptation is automatic through training.

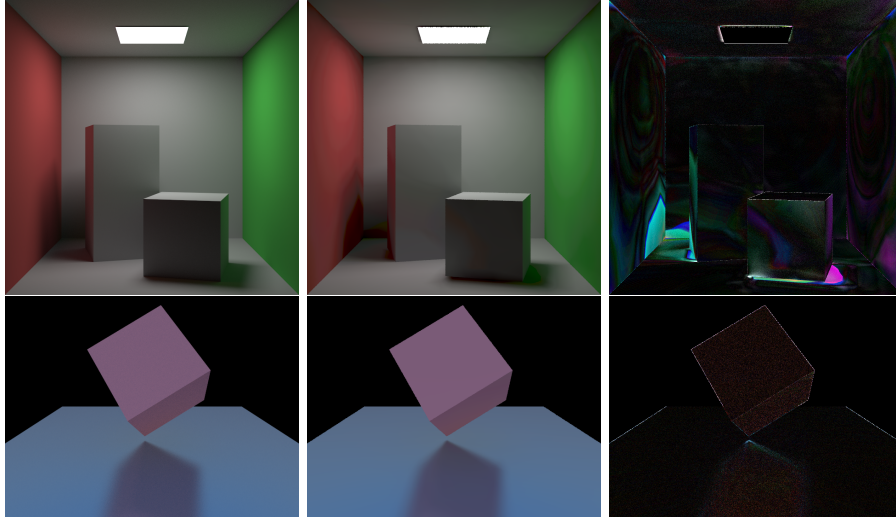


Figure 5: Approximation of the radiance $L(x, \omega)$ by artificial neural networks: The left column has been rendered by path tracing at 512 paths per pixel, while the middle column shows the approximation by artificial neural networks, and the right column visualizes their squared difference amplified by a factor of 10. The top row shows the diffuse Cornell box, while the bottom row features glossy reflections.

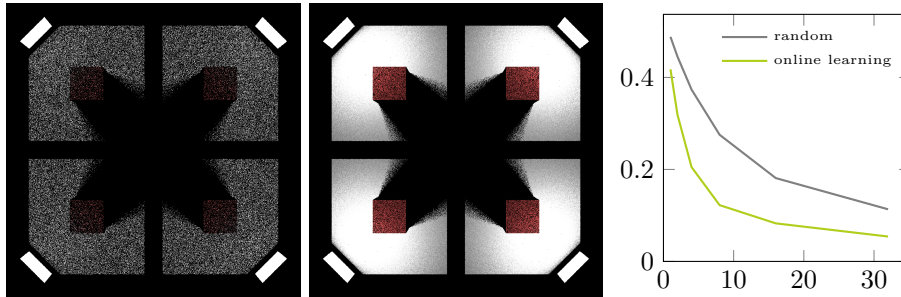


Figure 6: Both images on the left have been rendered at four samples per pixel. To render the left image we used random sampling for selecting a light source for next event estimation. The image in the middle was rendered using an artificial neural network trained online to select a light source with a high contribution to the point of intersection. The right image shows the relative root mean squared error (RMSE) of the two methods compared to a ground truth solution where the x-axis is the number of samples and the y-axis the RMSE.

The algorithm in Fig. 2 (see Sec.5.1) samples a density from the artificial neural network from which the cumulative distribution function is computed. This all can be avoided by using the artificial neural network to determine the parameters for an invertible function [27, 28]. The invertible function then is used to directly transform a set of uniform random numbers into a sample according to the learned density. Published during the revision of our manuscript, these techniques form the foundation of a new light transport path guiding al-

gorithm [29]. The article represents a big step forward in importance sampling, as for the first time it becomes possible to efficiently sample proportional to the solution of an integral equation.

Common to all approaches is the high cost of evaluating artificial neural networks, especially, when compared to techniques affordable in current games. A part of the performance gap can be addressed by using multiple small artificial neural networks instead of one large one [25]. Similar to splines, such an approach comes with competing goals: On the one hand, continuity across the artificial neural networks has to be established by overlapping supports. On the other hand, augmenting the number of input dimensions by what is called "one-hot encoding" or "one-blob encoding" [29], artificial neural networks automatically learn an adaptive representation instead of having to search for one.

Our initial experiments have been conducted for static scenes. Time can be added as another input dimension to the artificial neural networks as done in [26]. However, training an artificial neural network online in the style of [1, 29] is certainly more flexible. Combining the training algorithm presented in Sec.4 with the techniques from [29] may lead the path to real-time reinforcement learning (see Sec.2 and [1]) not only in computer graphics.

7. Conclusion

Building on the close relation of reinforcement learning and integral equations, a simple algorithm to train an artificial neural network to approximate the solution of an integral equation has been derived. Such a scheme provides a controlled environment that allows one to explore the smoothness of the progress of learning, suitable initializations of the artificial neural networks, and studying effects of regularization. In addition, a reference solution always can be computed and infinitely many training sets can be easily generated. This allows one to analyze the quality of the approximation by artificial neural networks and to potentially come up with a mathematical analysis along the lines of [30].

While high-dimensional function approximation in computer graphics becomes feasible by the application of artificial neural networks, their cost of evaluation is considerable. Therefore, future research will have to consider the complexity of artificial neural networks. Besides efficient algorithms to sample proportional to distributions controlled by artificial neural networks [27, 28, 29], function approximation by artificial neural networks may improve variance reduction based on the method of dependent tests, control variates, and the separation of the main part [31, 32, 33].

Acknowledgements

The authors thank Anton Kaplanyan, Thomas Müller, and Fabrice Rouselle for profound discussions and advice.

References

- [1] K. Dahm, A. Keller, Learning light transport the reinforced way, in: A. Owen, P. Glynn (Eds.), Monte Carlo and Quasi-Monte Carlo Methods. MCQMC 2016. Proceedings in Mathematics & Statistics, Vol. 241, Springer, 2018, pp. 181–195. [1](#), [2](#), [2](#), [3.2](#), [5.3](#), [6.4](#)
- [2] C. Browne, E. Powley, [A survey of Monte Carlo tree search methods](#), Intelligence and AI 4 (1) (2012) 1–49. doi:[10.1109/TCIAIG.2012.2186810](#). URL http://ieeexplore.ieee.org/xpls/abs_all.jsp?arnumber=6145622 [1](#)
- [3] I. Goodfellow, Y. Bengio, A. Courville, Deep Learning, MIT Press, 2016, <http://www.deeplearningbook.org>. [1](#), [3.2](#), [4](#), [5](#), [5.1](#)
- [4] D. Silver, J. Schrittwieser, K. Simonyan, I. Antonoglou, A. Huang, A. Guez, T. Hubert, L. Baker, M. Lai, A. Bolton, Y. Chen, T. Lillicrap, F. Hui, L. Sifre, G. van den Driessche, T. Graepel, D. Hassabis, Mastering the game of Go without human knowledge, Nature 550 (2017) 354–359. [1](#), [3](#), [3.2](#), [4](#)
- [5] M. Pharr, W. Jacob, G. Humphreys, Physically Based Rendering - From Theory to Implementation, Morgan Kaufmann, Third Edition, 2016. [2](#)
- [6] C. Watkins, P. Dayan, Q-learning, Machine learning 8 (3) (1992) 279–292. [2](#)
- [7] R. Sutton, Learning to predict by the methods of temporal differences, Machine Learning 3 (1) (1988) 9–44. [2](#)
- [8] L. Kocsis, C. Szepesvári, Bandit based Monte-Carlo planning, in: ECML-06. Number 4212 in LNCS, Springer, 2006, pp. 282–293. [3.1](#)
- [9] D. Silver, A. Huang, C. Maddison, A. Guez, L. Sifre, G. van den Driessche, J. Schrittwieser, I. Antonoglou, V. Panneershelvam, M. Lanctot, S. Dieleman, D. Grewe, J. Nham, N. Kalchbrenner, I. Sutskever, T. Lillicrap, M. Leach, K. Kavukcuoglu, T. Graepel, D. Hassabis, Mastering the game of Go with deep neural networks and tree search, Nature 529 (7587) (2016) 484–489. doi:[10.1038/nature16961](#). [3.2](#)
- [10] G. Tesauro, [Temporal difference learning and TD-Gammon](#), Commun. ACM 38 (3) (1995) 58–68. doi:[10.1145/203330.203343](#). URL <http://doi.acm.org/10.1145/203330.203343> [3.2](#)
- [11] D. Rumelhart, G. Hinton, R. Williams, Learning representations by back-propagating errors, in: J. Anderson, E. Rosenfeld (Eds.), Neurocomputing: Foundations of Research, MIT Press, Cambridge, MA, USA, 1988, pp. 696–699. [4](#), [5.1](#)

- [12] A. Keller, Quasi-Monte Carlo image synthesis in a nutshell, in: J. Dick, F. Kuo, G. Peters, I. Sloan (Eds.), Monte Carlo and Quasi-Monte Carlo Methods 2012, Springer, 2013, pp. 203–238. 4
- [13] J. Lehtinen, J. Munkberg, J. Hasselgren, S. Laine, T. Karras, M. Aittala, T. Aila, Noise2noise: Learning image restoration without clean data, Proc. International Conference on Machine Learning (ICML). 4
- [14] J. Traub, G. Wasilkowski, H. Woźniakowski, Information-Based Complexity, Academic Press, 1988. 4
- [15] M. Hessel, J. Modayil, H. van Hasselt, T. Schaul, G. Ostrovski, W. Dabney, D. Horgan, B. Piot, M. Azar, D. Silver, [Rainbow: Combining improvements in deep reinforcement learning](#), CoRR abs/1710.02298. [arXiv:1710.02298](#). URL <http://arxiv.org/abs/1710.02298> 5
- [16] V. Mnih, K. Kavukcuoglu, D. Silver, A. Graves, I. Antonoglou, D. Wierstra, M. Riedmiller, [Playing Atari with deep reinforcement learning](#), CoRR abs/1312.5602. URL <http://arxiv.org/abs/1312.5602> 5
- [17] R. Sutton, A. Barto, Introduction to Reinforcement Learning, 2nd Edition, MIT Press, Cambridge, MA, USA, 2017. 5
- [18] J. Halton, G. Weller, Algorithm 247: Radical-inverse quasi-random point sequence, Comm. ACM 7 (12) (1964) 701–702. 5.1
- [19] E. Veach, L. Guibas, Optimally combining sampling techniques for Monte Carlo rendering, in: SIGGRAPH '95 Proceedings of the 22nd annual conference on Computer graphics and interactive techniques, 1995, pp. 419–428. 5.3
- [20] E. Veach, Robust Monte Carlo Methods for Light Transport Simulation, Ph.D. thesis, Stanford University (1997). 5.3
- [21] R. Ramamoorthi, P. Hanrahan, An efficient representation for irradiance environment maps, in: Proceedings of the 28th Annual Conference on Computer Graphics and Interactive Techniques, SIGGRAPH '01, ACM, 2001, pp. 497–500. 6
- [22] R. Ng, R. Ramamoorthi, P. Hanrahan, [All-frequency shadows using non-linear wavelet lighting approximation](#), ACM Trans. Graph. 22 (3) (2003) 376–381. [doi:10.1145/882262.882280](#). URL <http://doi.acm.org/10.1145/882262.882280> 6
- [23] E. Lafortune, Y. Willems, A 5D tree to reduce the variance of Monte Carlo ray tracing, in: P. Hanrahan, W. Purgathofer (Eds.), Rendering Techniques 1995 (Proc. 6th Eurographics Workshop on Rendering), Springer, 1995, pp. 11–20. 6

- [24] T. Müller, M. Gross, J. Novák, Practical path guiding for efficient light-transport simulation, in: Proceedings of the Eurographics Symposium on Rendering, 2017, pp. 91–100. 6
- [25] P. Ren, J. Wang, M. Gong, S. Lin, X. Tong, B. Guo, [Global illumination with radiance regression functions](#), ACM Trans. Graph. 32 (4) (2013) 130:1–130:12. doi:10.1145/2461912.2462009. URL <http://doi.acm.org/10.1145/2461912.2462009> 6, 6.1, 6.4
- [26] P. Satýmýs, T. Bashford-Rogers, A. Chalmers, K. Debattista, A machine-learning-driven sky model, IEEE Computer Graphics and Applications (2017) 80–91. 6, 6.4
- [27] L. Dinh, D. Krueger, Y. Bengio, [NICE: non-linear independent components estimation](#), CoRR abs/1410.8516. arXiv:1410.8516. URL <http://arxiv.org/abs/1410.8516> 6.4, 7
- [28] L. Dinh, J. Sohl-Dickstein, S. Bengio, [Density estimation using real NVP](#), CoRR abs/1605.08803. arXiv:1605.08803. URL <http://arxiv.org/abs/1605.08803> 6.4, 7
- [29] T. Müller, B. McWilliams, F. Rousselle, M. Gross, J. Novák, [Neural importance sampling](#), CoRR abs/1808.03856. URL <https://arxiv.org/abs/1808.03856> 6.4, 7
- [30] K. Hornik, M. Stinchcombe, H. White, [Multilayer feedforward networks are universal approximators](#), Neural Netw. 2 (5) (1989) 359–366. doi:10.1016/0893-6080(89)90020-8. URL [http://dx.doi.org/10.1016/0893-6080\(89\)90020-8](http://dx.doi.org/10.1016/0893-6080(89)90020-8) 7
- [31] S. Heinrich, A Multilevel Version of the Method of Dependent Tests, in: Proc. of the 3rd St. Petersburg Workshop on Simulation, St. Petersburg University Press, 1998, pp. 31–35. 7
- [32] A. Keller, Hierarchical Monte Carlo image synthesis, Mathematics and Computers in Simulation 55 (1-3) (2001) 79–92. 7
- [33] F. Rousselle, W. Jarosz, J. Novák, Image-space control variates for rendering, ACM Transactions on Graphics (Proceedings of ACM SIGGRAPH Asia 2016) 35 (6) (2016) 169:1–169:12. doi:10.1145/2980179.2982443. 7